Extended Abstracts of the 2013 International Conference on Solid State Devices and Materials, Fukuoka, 2013, pp430-431

Strain Effect on Electronic Properties Tuning of Bilayer WS_2

Zheng Xin[1,2], Lang Zeng*, Kangliang Wei, Gang Du, Jinfeng Kang and Xiaoyan Liu*
[1] Key Laboratory of Microelectronic Devices and Circuits, Institute of Microelectronics, Peking University, 100871, P. R. China
[2] Peking University Shenzhen Graduate School, Shenzhen, 518055, P. R. China
* zenglang@ime.pku.edu.cn, xyliu@ime.pku.edu.cn

Abstract

Strain effect on the electronic properties of bilayer WS_2 is investigated by density functional theory (DFT). With biaxial strain, the band gap and carrier effective masses of AA and AB stacking bilayer WS_2 reduce with tensile biaxial strain. But their band gap increase first under small compressive strain and then decrease with larger compressive strain. This phenomenon can be understood by the detail of the electronic wave-function distribution and interplay of S_p- and W_d-orbits. The electronic properties of AA and AB stacking bilayer WS_2 with uniaxial strain are also studied.

1. Introduction

Recently transition metal dichalcogenides have attracted tremendous attentions. Among them, two-dimensional single/multi-layer MoS_2 were first fabricated and enormously investigated. However, several investigations suggested that WS_2 outperforms MoS_2 as the transistor channel material [1]. Hence, researches on WS_2 are in highly demand. In this paper, both biaxial and uniaxial strain is applied to AA and AB stacking bilayer WS_2 to the tuning of electronic properties. The first principles approach is used to investigate the strain effect. Electronic wave-function distribution and interplay of S_p- and W_d-orbits as well as carrier effective masses are analyzed. Based on the results, an integrated parameter is defined to explain the strain effect.

2. Calculation Method and Strain Model

Density Functional Theory approach (DFT) with ultra-soft pseudo-potential (USPP) implemented in CASTEP package was employed to perform the calculation. Exchange and correlation energy was approximated by generalized gradient approximation (GGA) with PW91. The energy cutoff for charge density was set to 600 eV. The van de walls interaction was also considered. Geometric optimization was completed until the maximum force was less than 0.02 eV/Å. The band gap of bulk WS_2 with lattice constant of a=3.153Å after relaxation was 0.97eV, which agrees well with previous work [2]. The AA and AB stacking bilayer WS_2 was constructed from bulk WS_2 (shown in Fig.1 (b) and (c)). Biaxial strain was applied to bilayer WS_2 with rhombus super-cell structure via changing the lattice constants as shown in Fig.1 (a). The rectangle super-cell of WS_2 was shown in Fig. 1 (d). The uniaxial strain was applied to bilayer WS_2 along x+y and x-y direction. The electronic properties affected by symmetrical biaxial strains were performed along irreducible path GMKG while asymmetrical uniaxial strains were calculated along GMKNLG shown in Fig.1 (e).

3. Results and Discussion

As shown in Fig. 2 and 4, AA stacking bilayer WS_2 has relatively larger band gap than AB stacking bilayer WS_2 due to different atoms arrangement. It can be seen from Fig.2 (b) the arrangement of AA stacking results in less electron overlap between two layers, which leads to larger band gap. For bilayer WS_2, the compressive biaxial strain makes Q valley lower than K point while the tensile strain lowers K valley [3]. This can be understood by the quantum quantization effect along layer thickness direction and consistent with the indirect-direct transition of monolayer MoS_2 [4]. The carrier effective masses reduce as tensile biaxial strain increases. However, under compressive strain, electron effective masses decrease but the tendency of hole effective masses is a little complex, related to the position of valence band maximum (VBM).

From Table.1, the thickness of bilayer WS_2 can be enlarged by compressive biaxial strain and then p-orbits of S atoms (S_p-orbits) contribute more than d-orbitals of W atoms (W_d-orbits) to conduction band minimum (CBM) and VBM. On the contrary, tensile biaxial strain decreases the thickness of bilayer WS_2 and W_d-orbits contribute more. This can be seen in Fig. 3 in which the electronic wave-function distribution at CBM and VBM of AB stacking bilayer WS_2 with ε=-9.6% and ε=10% respectively are plotted. The band gap of bilayer WS_2 decreases with increasing tensile biaxial strain. When compressive strain is applied, the band gap increases first and then decreases to 1.1eV and 1 eV, respectively for AA and AB stacking as shown in Fig.4. This can be understood by the interplay between S_p- and W_d-orbits. We define an integrated parameter N as follows, which can describe the S_p- and W_d-orbits interplay

$$N = \frac{\int f(E_d)dE}{\int f(E_p)dE} \qquad (1)$$

where $f(E_d)dE$ is the W_d-orbits contribution to electron wave function. N_CBM means this parameter is calculated near CBM.

The parameter N with various strains is plotted in Fig. 5. The larger the parameter, the more W_d-orbits like the electron state is. And larger integrated parameter N means lower CBM and VBM [5]. Thus if N_CBM decreases slower or increases faster than N_VBM, the band gap will decrease, but if N_CBM decreases faster than N_VBM the band gap will increase. It can be seen that the decreasing faster N_CBM than N_VBM in smaller compressive strain regime can explain the abnormal band gap increase in Fig. 4.

The influence of uniaxial strain to AA and AB stacking bilayer WS_2 is also investigated. The band structure and PDOS of strained AB stacking bilayer WS_2 are plotted in Fig.6. The uniaxial strain had similar modulation effect to bilayer WS_2 with biaxial strain. And it can be observed that the tuning effect of uniaxial strain is weaker than that of biaxial strain. With 10% tensile uniaxial strain, AB stacking bilayer WS_2 has band gap of 0.69 eV and 0.79 eV respectively for the uniaxial strain in x+y direction and x-y direction. The parameter N and carrier effective masses affected by uniaxial strain also have the alike tendency with those influenced by biaxial strain.

3. Conclusions

The electronic properties of both AA and AB stacking bilayer WS_2 affected by biaxial and uniaxial strain are studied. Tensile strain will reduce the band gap and carrier effective masses while small compressive strain will increase and large compressive strain will decrease the band gap. Analysis on electronic wave-function distribution and interplay of S_p- and W_d-orbits can be used to explain above results. This work can be a useful reference to broaden the application of strain engineering technology to WS_2 based electrical devices.

Acknowledgements

This work is supported by NSFC61250014.

References

[1] L. Liu, et.al, IEEE Trans. Electron Device, 58, 3042 (2011)
[2] Hong Jiang, Journal of Phys. Chem. C, 7664-7671 (2012)
[3] Hongliang Shi, et. al Phys. Rev. B, 87, 155304 (2012)
[4] Jason K. Ellis, et. al, Appl. Phys. Lett. 99, 261908 (2011)
[5] Swastubrata B., et. al, Phys. Rev. B.86.075454 (2012)

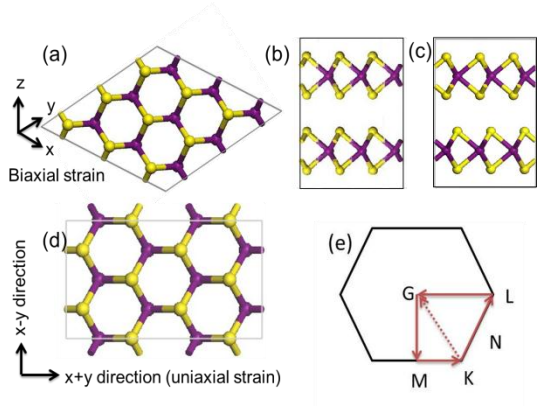

Fig.1 (a). Top view of WS_2 with rhombus super-cell. Biaxial strain is applied to bilayer WS_2 along both x and y direction. (b). AA stacking bilayer WS_2 (c). AB stacking bilayer WS_2, (d). Top view of WS_2 with rectangle super-cell. The uniaxial strain is applied respectively along x+y direction and x-y direction. (e). Irreducible Brillouin zone of WS_2 .Biaxial strains were performed along path GMKG while uniaxial strains were calculated along path GMKNLG. Red and yellow balls indicate W and S atoms.

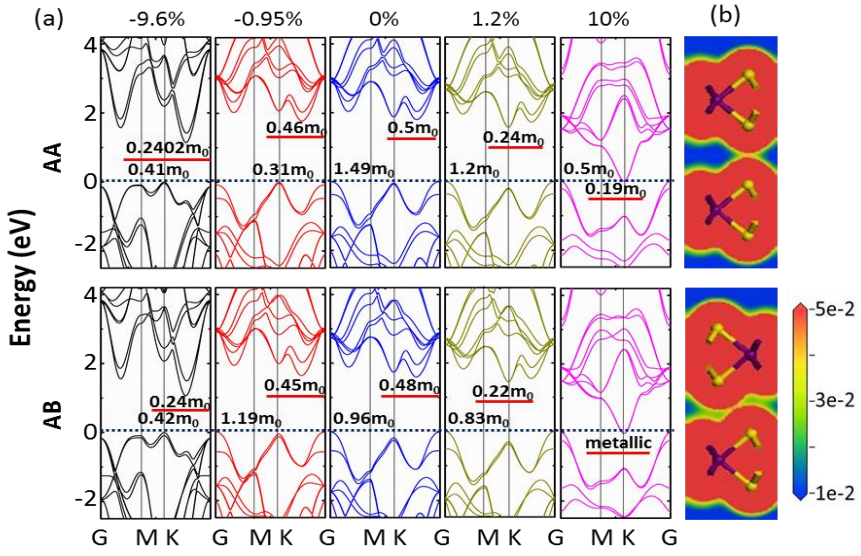

Fig.2 (a). Band structure of AA stacking and AB stacking bilayer WS_2 with biaxial strain, ε=-9.6% to 10%. And the carrier effective masses are also labeled. (b) and (c). Electron density of unstrained AA and AB stacking bilayer WS_2. The upper one is of AA stacking bilayer WS_2 and the lower one is of AB stacking one.

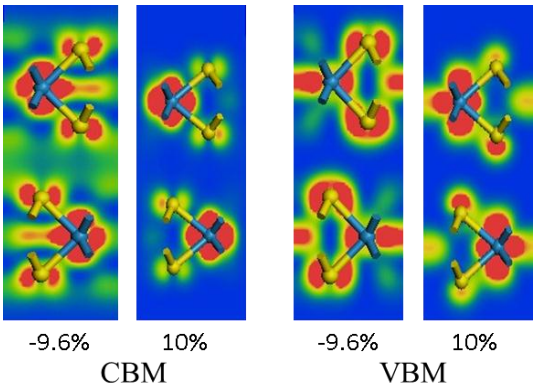

Fig.3 Wave function distribution of biaxial strained AB stacking bilayer WS_2 with ε=-9.6% and 10% at CBM and VBM.

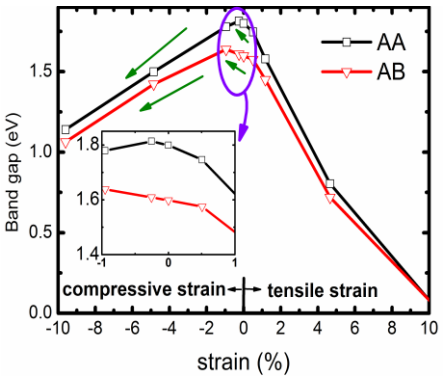

Fig.4 Band gap of AA stacking and AB stacking bilayer WS_2 with various biaxial strains. Insert figure is the magnified part in the purple circle.

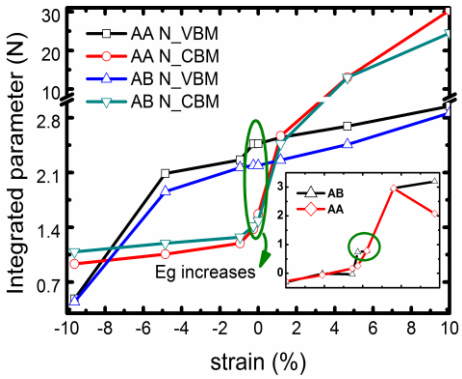

Fig.5 Integrated parameter N at CBM and VBM for AA and AB stacking bilayer WS_2 with different biaxial strain from -9.6% to 10%. Incell figure is the difference between slopes of N_CBM and N_VBM curves.

Table.1 distances between atoms in sandwich structure for biaxial strained bilayer WS_2 with various strains strength

Strain	-9.6%		-0.95%		0%		1.2%		10%	
Distance	$d_{W\text{-}S}$ (Å)	$d_{S\text{-}S}$ (Å)	$d_{W\text{-}S}$ (Å)	$d_{S\text{-}S}$ (Å)	$d_{W\text{-}S}$ (Å)	$d_{S\text{-}S}$ (Å)	$d_{W\text{-}S}$ (Å)	$d_{S\text{-}S}$ (Å)	$d_{W\text{-}S}$ (Å)	$d_{S\text{-}S}$ (Å)
AA stacking	2.367	3.401	2.404	3.180	2.410	3.158	2.417	3.132	2.492	2.965
AB stacking	2.366	3.400	2.404	3.179	2.408	3.163	2.417	3.132	2.491	2.963

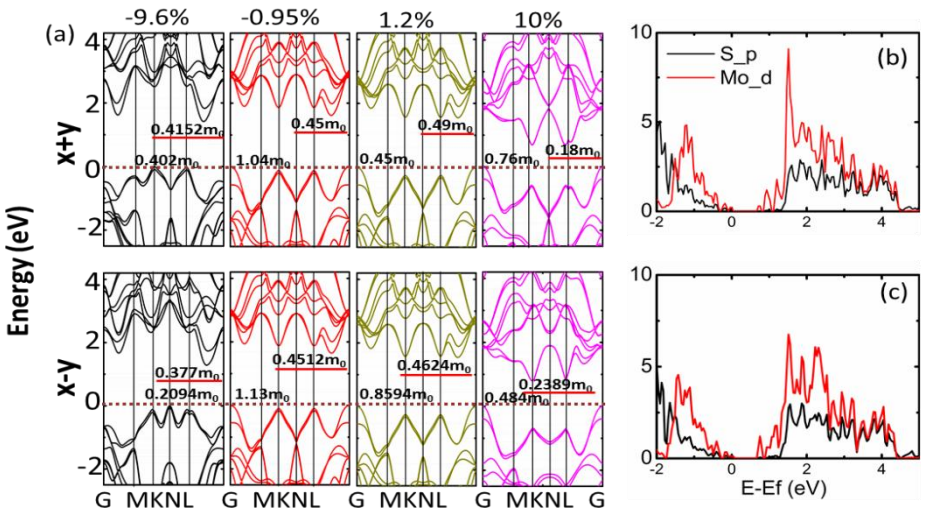

Fig.6 (a). Band structures along irreducible path of GMKNLG and carrier effective masses of AB stacking bilayer WS_2 with x+y and x-y direction uniaxial strain, ε=-9.6%, -0.95%, 1.2% and10% (b) and (c). PDOS of AB stacking bilayer WS_2 with uniaxial strain, ε=10% in x+y and x-y direction, respectively.

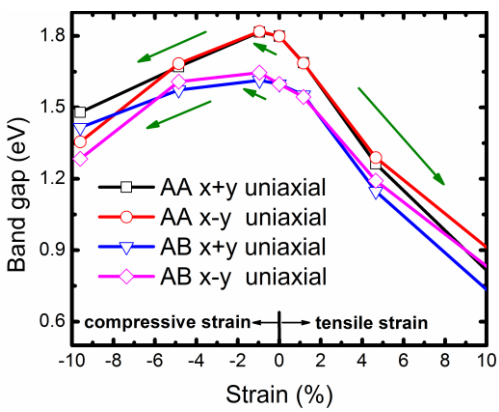

Fig.7 Bang gap of AA and AB stacking bilayer WS_2 with various uniaxial strain ε, from -9.6% to 10%. Similar tendency is observed. The band gap decreases with increasing tensile strain but increases first and then decreases with compressive strain.